Proceedings of the American Control Conference
San Diego, California • June 1999

Process Controller Design for Sheet Metal Forming

Cheng-Wei Hsu and A. Galip Ulsoy
Mechanical Engineering and Applied Mechanics
University of Michigan
Ann Arbor, MI 48109-2125, USA

Mahmoud Y. Demeri
Ford Research Laboratories
Ford Motor Company
Dearborn, MI 48121, USA

Abstract

In-process adjustment of the blank holder force can lead to higher formability and accuracy, and better part consistency. There are many studies on the application of process control to sheet metal forming. However, process controller design has not been thoroughly addressed, and is studied in this paper. A constant gain proportional plus integral (PI) controller with approximate inverse dynamics will be presented to achieve small tracking error regardless of model uncertainty and disturbances.

1 Introduction

Sheet metal stamping is an important manufacturing process because of its high speed and low cost for mass production. Figure 1 shows a schematic of a simplified stamping process.

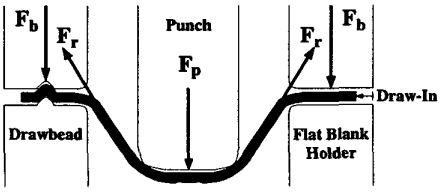

Figure 1: Schematic of a stamping process

The basic components are a punch, and a set of blank holders which may include drawbeads. The punch draws the blank to form the shape while the blank holder holds the blank to control the flow of metal into the die cavity. Some process variables are also shown: F_p is the punch force, F_b is the blank holder force, and F_r is the restraining force within the blank.

The good quality (i.e., no tearing, no wrinkling, and high dimensional accuracy) of stamped parts is critical in avoiding problems in assembly and in the final product performance. Consistency (i.e., dimensional variations between parts) in the stamping process also significantly affects subsequent assembly in mass production. New challenges emerge from the use of new materials. For example, lightweight materials (e.g., aluminum) are essential for reduction of car weight to achieve high fuel economy. However, aluminum has reduced formability and produces more springback [1, 2].

The control of flow of material into the die cavity is crucial to good part quality and consistency. Previous research showed that variable blank holder force during forming improves material formability [3, 4], reduces springback [1, 2, 5], and achieves part consistency [1, 2].

One strategy (i.e., process control) for the application of variable blank holder force is shown in Fig. 2 [1, 2].

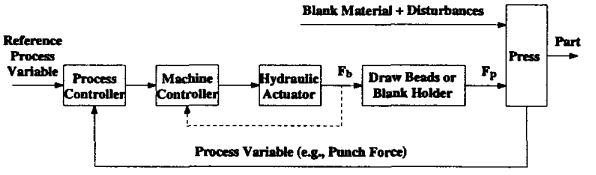

Figure 2: Process control of sheet metal forming

In this strategy, a measurable process variable (e.g., punch force) is controlled by following a predetermined (e.g., punch force-displacement) trajectory through manipulating the blank holder force. A similar approach has also been reported [5, 6, 7].

Recent work on process control in sheet metal forming led to the following conclusions [8]:

1. Consistency of part quality can be improved through the tracking property of feedback control.
2. Better part quality can be achieved through selection of the reference punch force trajectory.

It is important to realize that a badly designed process controller cannot ensure good tracking performance, and, in turn, cannot guarantee good part quality and consistency. Clearly, the process controller plays an important role in the feedback control system and needs further investigation.

Issues of process controller design for sheet metal forming have not been properly addressed, especially, from a control point of view. Modeling sheet metal forming for process controller design has been investigated [9]. Hsu *et al.* [10] recently proposed a first-order non-linear dynamic model for u-channel forming which can capture the main characteristics of the process dynamics observed during experiments. Proportional plus integral (PI) control has been used for sheet metal forming and controller parameters were typically determined by trial and error [11].

The disadvantage of PI control is that high controller gains can achieve good tracking performance but cannot maintain good stability robustness while low controller gains can maintain good stability robustness but cannot achieve good tracking performance. Since sheet metal forming is a highly nonlinear process, it is difficult to tune a PI controller to stabilize the closed-loop system with good tracking performance. Hsu

et al. [8] investigated constant gain PI control with feedforward action (PIF). Although PIF control worked well under dry condition, it generated a huge peak in the blank holder force under lubricated condition.

The purpose of this investigation is to systematically develop a process controller for sheet metal forming to stabilize the closed-loop system with good tracking performance. A constant gain PI process controller with approximate inverse dynamics for sheet metal forming will be proposed. The first-order non-linear dynamic model for u-channel forming [10] will be explored to obtain the approximate inverse dynamics, which is related to tracking performance. The constant gain PI control will be designed to ensure the tracking performance regardless of disturbance and model uncertainty. Numerical simulation results will demonstrate the capabilities of the proposed controller.

2 Systematic Process Controller Design

A schematic of the constant gain PI controller with inverse dynamics is shown in Fig. 3. The block "Plant" refers

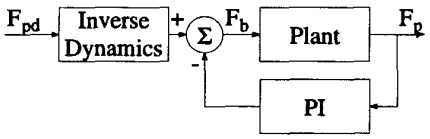

Figure 3: Schematic of the constant gain PI controller with inverse dynamics.

to the real stamping process or its process model. F_{pd} is the reference punch force trajectory, F_b is the blank holder force applied to the plant, and F_p is the punch force generated by the plant. A systematic development of the proposed controller requires the following steps:

1. Model sheet metal forming (i.e., "Plant") for process controller design.
2. Design the process controller (i.e., "Inverse Dynamics" and "PI").
3. Adjust and test the performance of the process controller through simulation.
4. Adjust and verify the performance of the process controller through experiment.

Adjustment and verification of the performance of the process controller will not be presented in this paper.

2.1 Modeling of Sheet Metal Forming

The process model for u-channel forming can be represented by the following first-order non-linear dynamic model [8, 10]:

$$\dot{F}_p = -\frac{1}{\tau(F_b)}F_p + \frac{\alpha(F_b)}{\tau(F_b)}F_b + \frac{\partial F_{pc}}{\partial F_b}\dot{F}_b \tag{1}$$

where

$$F_{pc} = \alpha(F_b)\cdot F_b \cdot (1-\exp(-\frac{t}{\tau(F_b)})) \tag{2}$$

$$\alpha(F_b) = 1.3537 - 1.8511\times 10^{-2}\cdot F_b + 1.2340\times 10^{-4}\cdot F_b^2 \tag{3}$$

$$\tau(F_b) = 1.5689 + 5.6906\times 10^{-2}\cdot F_b - 1.2669\times 10^{-3}\cdot F_b^2 + 1.0279\times 10^{-5}\cdot F_b^3 \tag{4}$$

$\alpha(F_b)$ and $\tau(F_b)$ are the DC gain and the time constant, derived from constant blank holder force experiments.

2.2 Design of the Constant Gain PI Controller with Approximate Inverse Dynamics

For a given reference punch force trajectory, a controller is designed to generate the blank holder force to achieve:

1. Stabilization of the closed-loop system.
2. Asymptotic convergence of the punch force and the reference punch force trajectory.

The proposed controller consists of two parts: approximate inverse dynamics and PI control. The approximate inverse dynamics tracks the reference trajectory while the PI control ensures good tracking performance regardless of disturbance and model uncertainty.

2.2.1 Approximate Inverse Dynamics: A schematic of the inverse dynamics is shown in Fig. 4. F_{b0} is the out-

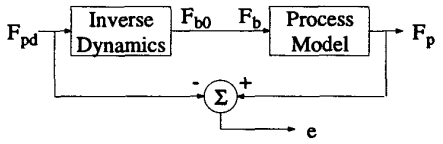

Figure 4: Schematic of the inverse dynamics.

put of the inverse dynamics and also part of the calculated blank holder force through the proposed controller, and e is the tracking error due to using the inverse dynamics alone. In fact, the inverse dynamics is feedforward control.

The tracking error is defined by

$$e(t) = F_p(F_b,t) - F_{pd}(t) \tag{5}$$

The tracking error dynamics, obtained from the derivative of $e(t)$ with respect to time, t, and the substitution of Eq. 1, becomes

$$\dot{e} = -\frac{1}{\tau(F_b)}e + \frac{\alpha(F_b)}{\tau(F_b)}F_b + \frac{\partial F_{pc}(F_b,t)}{\partial F_b}\dot{F}_b - \dot{F}_{pd} - \frac{1}{\tau(F_b)}F_{pd} \tag{6}$$

Lyapunov theorem is applied to prove the asymptotic stability of the tracking error dynamics, which means asymptotic convergence of e to zero. Choose a candidate Lyapunov function as

$$V = \frac{1}{2}e^2 \tag{7}$$

Its derivative with respect to t is

$$\dot{V} = -\frac{1}{\tau(F_b)}e^2 + e\left[\frac{\alpha(F_b)}{\tau(F_b)}F_b + \frac{\partial F_{pc}(F_b,t)}{\partial F_b}\dot{F}_b - \dot{F}_{pd} - \frac{1}{\tau(F_b)}F_{pd}\right] \tag{8}$$

If

$$\frac{\partial F_{pc}(F_b,t)}{\partial F_b}\dot{F}_b + \frac{\alpha(F_b)}{\tau(F_b)}F_b = \dot{F}_{pd} + \frac{1}{\tau(F_b)}F_{pd} \tag{9}$$

then Eq. 8 becomes

$$\dot{V} = -\frac{1}{\tau(F_b)} V \tag{10}$$

Equation 10 is negative definite because $\tau(F_b) > 0$ [10]. According to Lyapunov theorem, the tracking error dynamics is asymptotically stable if Eq. 9 is satisfied. Therefore, Eq. 9 is the inverse dynamics since F_b can be solved for a given F_{pd}. Solving F_b from Eq. 9 depends on $\frac{\partial F_{pc}(F_b,t)}{\partial F_b}$ because $\frac{\partial F_{pc}(F_b,t)}{\partial F_b}$ could be zero. Figure 5 shows contours of $\frac{\partial F_{pc}(F_b,t)}{\partial F_b}$. The

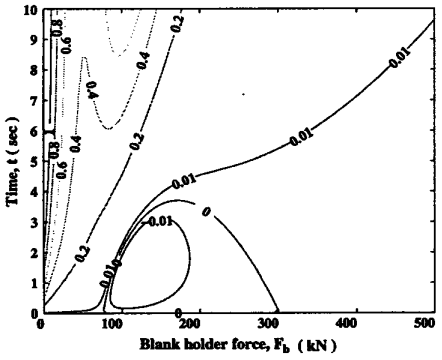

Figure 5: Contours of $\frac{\partial F_{pc}(F_b,t)}{\partial F_b}$.

figure shows that $\frac{\partial F_{pc}(F_b,t)}{\partial F_b}$ could be zero. This will cause numerical problems about solving F_b, because $\dot{F}_b$ could be very large or become indeterminable, which implies that F_b will change abruptly or cannot be found. To reconcile this problem, that $\dot{F}_b = 0$ when $\left|\frac{\partial F_{pc}(F_b,t)}{\partial F_b}\right| < 10^{-2}$ will be assumed in simulation. The inverse dynamics (i.e., Eq. 9) with this assumption will be called the approximate inverse dynamics. Later, F_{b0} will denote the solution of Eq. 9.

2.2.2 Constant Gain PI Control: Generally, the inverse dynamics or the feedforward control cannot sustain any disturbance or model uncertainty. A feedback control using a constant gain PI controller is built to reject disturbance and improve robustness to model uncertainty. The constant gain PI controller is designed based on the perturbed process model.

The perturbed process model is derived as follows. Assuming that the disturbance, F_d, comes at the input of the process model in Fig. 4, then

$$F_b = F_{b0} + F_d \tag{11}$$

The tracking error, ε, becomes

$$\varepsilon = F_p(F_b,t) - F_{pd} \tag{12}$$

ε consists of e and the error due to F_d. Assuming that F_d is much smaller than F_{b0}, then $F_p(F_b,t)$ in Eq. 12 can be approximated by

$$F_p(F_b,t) \simeq F_p(F_b,t)\Big|_{F_b=F_{b0}} + \frac{\partial F_{pc}(F_b,t)}{\partial F_b}\Big|_{F_b=F_{b0}} \cdot F_d - F_{pd} \tag{13}$$

where $\frac{\partial F_p}{\partial F_b} \simeq \frac{\partial F_{pc}}{\partial F_b}$ is applied [10]. Substituting Eq. 13 into Eq. 12 leads to

$$\varepsilon = e + \frac{\partial F_{pc}(F_b,t)}{\partial F_b}\Big|_{F_b=F_{b0}} \cdot F_d \tag{14}$$

Although e decays asymptotically, ε is still influenced by F_d. The perturbed process model is

$$\varepsilon_d = \frac{\partial F_{pc}(F_b,t)}{\partial F_b}\Big|_{F_b=F_{b0}} \cdot F_d \tag{15}$$

To maintain tracking performance (i.e., ε approaches e), a feedback loop is designed to force ε_d to converge to zero. A constant gain PI controller is investigated here. Figure 6 shows the block diagram. K_p is the proportional gain and

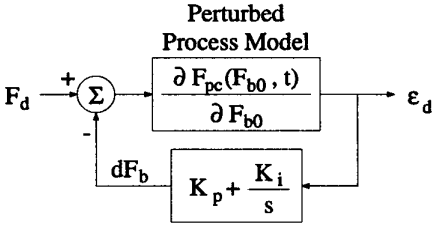

Figure 6: Block diagram for feedback loop design.

K_i is the integral gain. dF_b is the output of the PI controller and also part of the calculated blank holder force through the proposed controller.

Assuming that the perturbed process model is a constant gain, G_0, then for the constant gain PI controller, the dynamic equation of the closed-loop system becomes

$$\dot{\varepsilon_d} + \frac{G_0 K_i}{1 + G_0 K_p} \varepsilon_d = \frac{G_0}{1 + G_0 K_p} \dot{F}_d \tag{16}$$

Its solution is

$$\varepsilon_d(t) = \varepsilon_d(0) \exp\left(\frac{-t}{\tau_0}\right) + \int_0^t \exp\left(\frac{\tau - t}{\tau_0}\right) \frac{\dot{F}_d(\tau)}{\tau_0 K_i} d\tau \tag{17}$$

where

$$\tau_0 = \frac{1 + G_0 K_p}{G_0 K_i} \tag{18}$$

τ_0 is the time constant and τ is the dummy variable. For a given G_0, choose K_i and K_p such that τ_0 is as small as possible and $\tau_0 K_i$ as large as possible. Hence, ε_d will decrease as quickly as possible. However, ε_d generally depends on F_d.

2.3 Constant Gain PI Controller with Approximate Inverse Dynamics

The block diagram for the constant gain PI controller with approximate inverse dynamics is shown in Fig. 7.

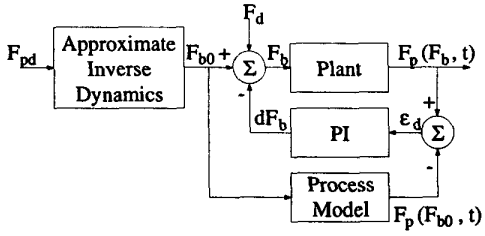

Figure 7: Block diagram for the constant gain PI controller with approximate inverse dynamics.

3 Simulations and Results

The simulation is used to show the performance of the proposed controller on disturbance rejection and robustness to model uncertainty. In the following simulations, the reference punch force trajectory, F_{pd}, is generated by Eq. 1 using the constant blank holder force, 60 kN.

3.1 No Disturbance and No Model Uncertainty

F_d in Fig. 7 is 0 kN. The mathematical relations for the blocks of "Plant" and "Process Model" in Fig. 7 are identical. Figure 8 shows the simulation results. Figure (a) shows that

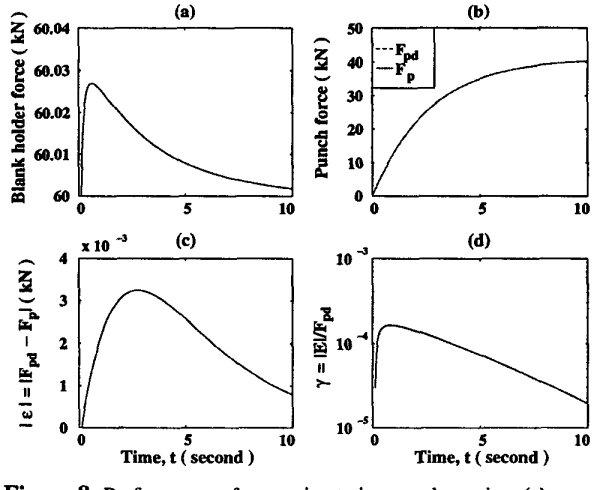

Figure 8: Performance of approximate inverse dynamics: (a) measured F_b (i.e., F_b), (b) reference F_p (i.e., F_{pd}) and measured F_p (i.e., F_p), (c) tracking error, $|\varepsilon| = |F_p - F_{pd}|$, and (d) relative tracking error, $\gamma = |\varepsilon|/F_{pd}$.

F_b is very close to 60 kN. The maximum overshoot is less than 0.03 kN. The reasons for $F_b \neq 60$ kN are the previously mentioned numerical problem (i.e., when $\left|\frac{\partial F_{pc}(F_b,t)}{\partial F_b}\right| \ll 1$, F_b changes abruptly or cannot be found) and calculation errors. Figure (b) shows that F_p can track F_{pd} very well. Figures (c) and (d) show very low tracking error (less than 4×10^{-3} kN) and relative tracking error (less than 2×10^{-4}).

3.2 Disturbance Rejection

F_d in Fig. 7 is set to be 20 kN. The mathematical relations for the blocks of "Plant" and "Process Model" in Fig. 7 are identical. Figure 9 shows the simulation results. Figure (a) shows

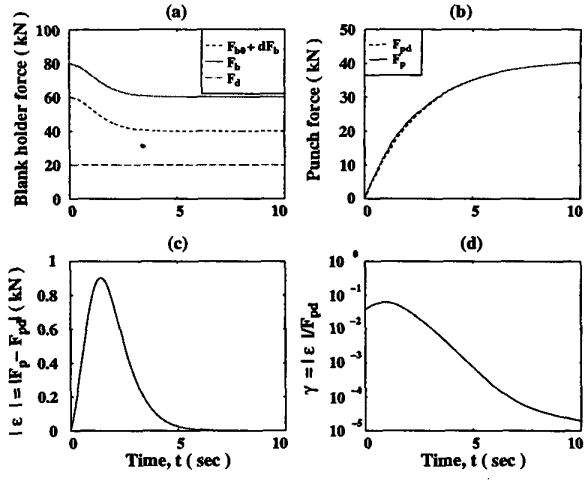

Figure 9: Performance of disturbance rejection: (a) calculated F_b (i.e., $F_{b0} + dF_b$), measured F_b (i.e., F_b), and disturbance (i.e., F_d), (b) reference F_p (i.e., F_{pd}) and measured F_p (i.e., F_p), (c) tracking error, $|\varepsilon| = |F_p - F_{pd}|$, and (d) relative tracking error, $\gamma = |\varepsilon|/F_{pd}$.

that the controller output (i.e., $F_{b0} + dF_b$) can be adjusted to compensate the disturbance; therefore, the measured F_b finally approaches 60 kN. Figure (b) shows that F_p can track F_{pd} regardless of disturbance, F_d. The tracking error, ε, in Fig. (c) asymptotically decays and its maximum value is up to 0.9 kN. The relative error, γ, in Fig. (d) also asymptotically decays. After 5 sec, the relative error is less than 10^{-3}.

3.3 Robustness to Model Uncertainty

F_d in Fig. 7 is set to be 0 kN. The uncertainty is shown by varying model parameters in "Plant":

$$\alpha(\text{"Plant"}) = (1+\delta_\alpha)\cdot\alpha(\text{"Process Model"}) \quad (19)$$

$$\tau(\text{"Plant"}) = (1+\delta_\tau)\cdot\tau(\text{"Process Model"}) \quad (20)$$

Figure 10 shows the simulation results for $\delta_\alpha = 0.1$ and $\delta_\tau = 0.1$. Figure (a) shows the measured F_b, which is in fact the same as the controller output (i.e., $F_{b0} + dF_b$). The measured F_b or the controller output can be adjusted to compensate model uncertainty. Figure (b) shows that F_p can track F_{pd} regardless of model uncertainty. Figure (b) shows that F_p can track F_{pd} regardless of disturbance, F_d. The tracking error, ε, in Fig. (c) asymptotically decays and its maximum value is up to about 0.2 kN. The relative error, γ, in Fig. (d) also asymptotically decays. It is less than 0.01.

4 Discussion

In Fig. 5, the area where $\left|\frac{\partial F_{pc}(F_b,t)}{\partial F_b}\right| > 0.01$ allows $\dot{F}_b$ not to be zero while the area where $\left|\frac{\partial F_{pc}(F_b,t)}{\partial F_b}\right| \leq 0.01$ assumes $\dot{F}_b$ to be zero. This assumption in fact limits the upper bound of $|\dot{F}_b|$. According to this assumption, the approximate inverse

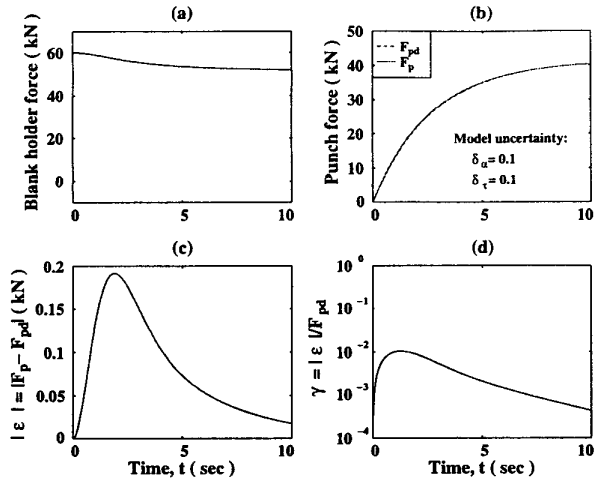

Figure 10: Performance of robustness to model uncertainty ($\delta_\alpha = 0.1$ and $\delta_\tau = 0.1$): (a) measured F_b, (b) reference F_p (i.e., F_{pd}) and measured F_p (i.e., F_p), (c) tracking error, $|\varepsilon| = |F_p - F_{pd}|$, and (d) relative tracking error, $\gamma = |\varepsilon|/F_{pd}$.

dynamics can successfully generate a blank holder force trajectory (i.e., F_{b0}) corresponding to a given reference punch force trajectory.

The tracking error, ε, can be divided into two parts: e due to the inverse dynamics and ε_d due to the disturbance. (See Eqs. 14 and 15.) When there is no disturbance and no model uncertainty, ε is in fact the same as e. When there is disturbance or model uncertainty, ε will be larger than e. For example, Figs. 9(c) and 10(c) show larger tracking errors than Fig. 8(c). Therefore, the inverse dynamics will determine the tracking performance.

As shown in Fig. 4, the inverse dynamics is actually feedforward control; therefore, it cannot maintain its performance when disturbance or model uncertainty appears. The feedback control (i.e., the constant PI controller) is designed to maintain the tracking performance regardless of disturbance or model uncertainty. Although the tracking errors in Figs. 9(c) and 10(c) are larger than the tracking error in Fig. 8(c), they decay asymptotically. Therefore, the tracking performance can be maintained through the constant PI controller regardless of disturbance or model uncertainty.

5 Summary and Conclusions

A constant gain PI controller with approximate inverse dynamics is systematically designed based on the first-order non-linear dynamics. The proposed controller has a feedforward loop (i.e., the approximate inverse dynamics) and a feedback loop (i.e., the constant gain PI control). The feedforward loop determines the tracking performance while the feedback loop relates to disturbance rejection and robustness to model uncertainty. Simulation shows that the proposed controller can track the reference regardless of disturbance and model uncertainty. Future work will include experimental implementation and validation of the proposed controller.

Acknowledgements

The authors gratefully acknowledge the technical and financial support provided by the Ford Motor Company.

References

[1] Adamson, A. M., 1995, "Closed-Loop Dimensional Control in Sheet Metal Forming via the Blank Restraining Force", M.S. thesis, University of Michigan, Ann Arbor, MI.

[2] Adamson, A., Ulsoy, A. G., and Demeri, M., 1996, "Dimensional Control in Sheet Metal Forming via Active Binder Force Adjustment," *SME Transactions*, Vol. 24, pp. 167-178.

[3] Ahmetoglu, M., Broek, T. R., Kinzel, G., and Altan, T., 1995, "Control of Blank Holder Force to Eliminate Wrinkling and Fracture in Deep-Drawing Rectangular Parts," *CIRP Annals*, Vol. 44, No. 1, pp. 247-250.

[4] Jalkh, P., Cao, J., Hardt, D., and Boyce, M. C., 1993, "Optimal Forming of Aluminum 2008-T4 Conical Cups Using Force Trajectory Control," *SAE Technical Paper No. 930286.*

[5] Sunseri, M., Karafillis, A. P., Cao, J., and Boyce, M. C., 1994, "Methods to Obtain Net Shape in Aluminum Sheet Forming Using Active Binder Force Control," AMD–Vol. 194, *Mechanics in Materials Processing and Manufacturing*, ASME, pp. 167-184.

[6] Hardt, D. E. and Fenn, R. C., 1993, "Real-Time Control of Sheet Stability during Forming," *Transactions of the ASME, Jorunal of Engineering for Industry*, Vol. 115, pp. 299-308.

[7] Siegert, K., Wagner, S., and Ziegler, M., 1996, "Closed Loop Binder Force System," *SAE Technical Paper No. 960824.*

[8] Hsu, C.-W., Demeri, M. Y., and Ulsoy, A. G., 1999, "Improvement of Consistency in Stamped Part Quality Using Process Control," *1999 TMS Annual Meeting: Sheet Metal Forming Technology*, February 28 - March 4, 1999, San Diego, California.

[9] Majlessi, S. A., Kashani, A. R., and Weinmann, K. J., 1992, "Stamping Process Modelling for Real-Time Control," *Transactions of NAMRI/SME*, Vol. XX, pp. 33-38.

[10] Hsu, C.-W., Ulsoy, A. G., and Demeri, M. Y., 1998, "Modeling for Control of Sheet Metal Forming," *Proceedings of 1998 Japan-USA Symposium on Flexible Automation*, Otsu, Japan, pp. 1143-1148.

[11] M. Sunseri, J. Cao, A. P. Karafillis, and M. C. Boyce, "Accommodation of Springback Error in Channel Forming Using Active Binder Force Control: Numerical Simulation and Experiments," *Transactions of the ASME, Journal of Engineering Materials and Technology*, Vol. 118, pp. 426-435, July 1996.